HHS Public Access

Author manuscript

J Am Chem Soc. Author manuscript; available in PMC 2024 May 24.

Published in final edited form as:

J Am Chem Soc. 2023 May 24; 145(20): 11056–11066. doi:10.1021/jacs.3c00165.

Global discovery of covalent modulators of ribonucleoprotein granules

Anthony M. Ciancone[1,#], **Kyung W. Seo**[5,#], **Miaomiao Chen**[1,#], **Adam L. Borne**[2], **Adam H. Libby**[1,4], **Dina L. Bai**[1], **Ralph E. Kleiner**[*,5], **Ku-Lung Hsu**[*,1,2,3,4]

[1]Department of Chemistry, University of Virginia, Charlottesville, Virginia 22904, United States

[2]Department of Pharmacology, University of Virginia School of Medicine, Charlottesville, Virginia 22908, United States

[3]Department of Molecular Physiology and Biological Physics, University of Virginia, Charlottesville, Virginia 22908, United States

[4]University of Virginia Cancer Center, University of Virginia, Charlottesville, VA 22903, USA

[5]Department of Chemistry, Princeton University, Princeton, NJ 08544, USA

Abstract

Stress granules (SGs) and processing-bodies (PBs, P-bodies) are ubiquitous and widely studied ribonucleoprotein (RNP) granules involved in cellular stress response, viral infection, and the tumor microenvironment. While proteomic and transcriptomic investigation of SGs and PBs have provided insights into molecular composition, chemical tools to probe and modulate RNP granules remain lacking. Herein, we combine an immunofluorescence-based phenotypic screen with chemoproteomics to identify sulfonyl-triazoles (SuTEx) capable of preventing or inducing SG and PB formation through liganding of tyrosine and lysine sites in stressed cells. Liganded sites were enriched for RNA-binding and protein-protein interaction domains, including several sites found in RNP granule-forming proteins. Among these, we functionally validate G3BP1 Y40, located in the NTF2 dimerization domain, as a ligandable site that can disrupt arsenite-induced SG formation in cells. In summary, we present a chemical strategy for the systematic discovery of condensate-modulating covalent small molecules.

Graphical Abstarct:

[*]Authors to whom correspondence should be addressed: kenhsu@virginia.edu (K.-L.H.), Department of Chemistry, Department of Pharmacology, University of Virginia, McCormick Road, P.O. Box 400319, Charlottesville, VA 22904, Phone: 434-297-4864, rkleiner@princeton.edu (R.E.K.), Department of Chemistry, Princeton University, 359 Frick Chemistry Laboratory, Washington Road, Princeton, NJ 08544, Phone: 609-258-1654.

[#]These authors contributed equally

Competing Interests

K.-L.H. is scientific founder and advisor to Umbra Therapeutics

EXPERIMENTAL METHODS

Detailed methods are provided in the Supporting Information

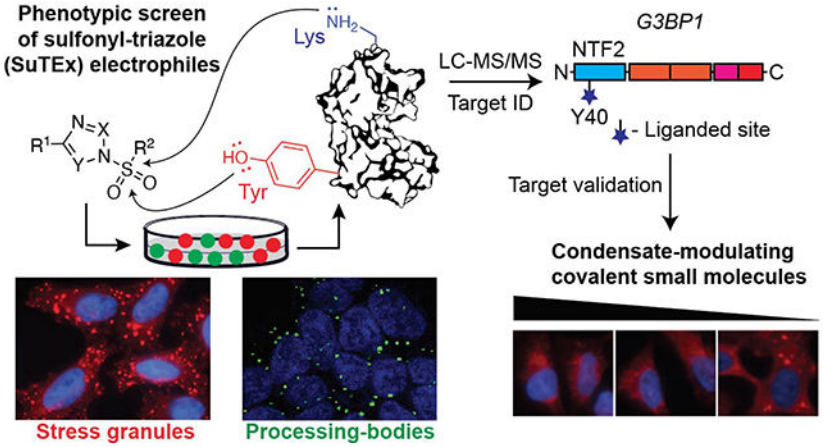

Keywords

SuTEx; stress granules; P-bodies; LLPS; biomolecular condensates; chemoproteomics; ribonucleoprotein; granules; activity-based protein profiling

INTRODUCTION

Cellular RNA and protein accumulate in membraneless subcellular compartments referred to collectively as biomolecular condensates[1]. Condensate formation is proposed to involve liquid-liquid phase separation (LLPS) of proteins and nucleic acids, can occur in response to cellular stimuli, and is associated with the regulation of RNA metabolism, translation, and signal transduction[1–2]. Stress granules (SGs) and processing bodies (PBs) are widely studied cytoplasmic ribonucleoprotein (RNP) granules that are implicated in post-transcriptional control of gene expression and cellular fitness although their specific functions remain to be fully elucidated[2a].

SG and PB formation is driven by key granule-forming RNA-binding proteins (RBPs). These RNPs can self-organize into granule structures through protein-RNA, protein-protein and RNA-RNA interactions to mediate multiphase condensation[2a, 3]. Cells form SGs under stress conditions while PBs exist constitutively but can increase in size and number with stress[2a, 4]. SG formation is triggered by the integrated stress response through activation of kinases that phosphorylate eIF2α, resulting in translational arrest and accumulation of untranslated mRNA that promote protein and RNA condensation[2a, 5]. The SG-associated proteome includes proteins involved in RNA metabolism, mRNA translation and essential SG-nucleating RBPs[2a, 3a, b, 6] (e.g., Ras GTPase-activating protein-binding protein or G3BP). PBs are enriched for proteins involved in mRNA decay including mRNA-decapping enzymes (DCP1A and DCP2) and enhancer of mRNA-decapping proteins (EDC3 and EDC4)[7].

Aberrant regulation of RNP granules has been associated with an increasing number of disease states[8]. Cancer resistance to radiation or chemotherapeutics has been linked to formation of pro-survival SGs[9]. PBs are reported to be regulated by alpha-synuclein, an

aggregating protein genetically linked to Parkinson's disease[10]. More generally, the ability to pharmacologically modulate disease-relevant condensates may provide new therapeutic opportunities but has so far proven challenging to identify compounds that directly engage granule forming proteins or RNA[11]. One of the barriers is the difficulty in targeting the RNA binding interface of granule forming RBPs using small molecules because of the large, buried surface area and prevalence of positively charged amino acids in RNA-binding domains[12] (RBDs). RBPs also contain intrinsically disordered regions (IDRs) involved in RNA binding that have been historically difficult to target with small molecules[13].

Pharmacological modulation of RNP granules has been primarily achieved through perturbation of major upstream biological processes leading to condensation. As such, these compounds affect multiple cellular pathways and are often unsuitable as specific modulators of RNP condensates due to off-target effects and cytotoxicity. General inhibitors of translational elongation (e.g., emetine and cycloheximide) have been used to disassemble SGs and stress-induced PBs[3f, 14]. Toxins including pateamine A and hippuristanol can induce SGs in an eIF2α-independent manner by inactivating the RNA helicase eIF4A[3f, 15]. Chemotherapy can trigger PB[16] and SG formation[7a, 8f, 9d, e]. High-throughput screening (HTS) has been pursued and while promising, the mode of action for these condensate-modulating compounds remains ill-defined[17]. Compounds that target SG proteins have been reported but direct binding remains to be demonstrated[18]. Thus, apart from approved drugs with condensate modifying activity discovered after the fact[19], RNP granule modulators consist largely of toxic compounds or lead hits from HTS that lack known direct binding targets.

Here, we discovered a suite of electrophilic sulfonyl-triazole (SuTEx) compounds that modulate SG and PB levels in cells through covalent binding to central granule-forming RBPs. Active compounds from phenotypic screening were subjected to competitive activity-based protein profiling (ABPP) and quantitative proteomics to identify a collection of ~300 protein targets replete with ligandable tyrosine and lysine sites (>770 in aggregate). A substantial fraction of liganded proteins (~38%) were previously identified in proteomic analyses of RNP granules that included SG-nucleating (G3BP1) and PB-enhancing (EDC3) components. Importantly, we functionally validated G3BP1 Y40 as a ligandable site necessary for the SG-inhibitory activity of HHS-166 in oxidatively stressed cells. Our findings support covalent binding at tyrosine and lysine residues as a global strategy for discovery of RNP granule modifiers.

RESULTS

Phenotypic screening for RNP-granule-modulating SuTEx compounds

We reasoned screening of tyrosine (Tyr)- and lysine (Lys)-reactive electrophiles would facilitate discovery of RNP granule modulators due to the prevalence of these residues in protein-RNA interfaces (PRI; 2 and 6 residues/PRI, respectively[12]). Cysteines (Cys), by contrast, are found at a much lower frequency in PRIs (<1 residue/PRI), which further supports exploration of Tyr/Lys- vs Cys-targeting for the initial electrophile screen. Although sulfonyl-fluorides (SuFEx[20]) and -triazoles (SuTEx) both function as Tyr/Lys-binding electrophiles, we chose the latter because of capabilities for tuning reactivity

and affinity though leaving group (LG) modifications[21] (Figure 1A and S1). Importantly, SuTEx probe binding activity in cells identified enrichment for RBD and protein-protein interaction (PPI) domains that are commonly found on RNP granule proteins (e.g., RRM and SH3 domains, respectively)[7b, 22]. HEK293T and HeLa cells were chosen for screening and downstream analyses because these cell lines have served as model systems for cell biological and proteomic evaluation of PBs and SGs[7b, 8h, 10, 23].

We used immunofluorescence (IF) detection for phenotypic screening of SuTEx compound activity on stress-induced PB and SG levels in cells (Figure 1B). PBs were induced through glucose deprivation of HEK293T cells and detected by immunofluorescence with anti-enhancer of mRNA-decapping protein 4 (EDC4) as previously described[3f, 23a] (~4 vs 2 PBs/cell in -glucose and +glucose conditions, respectively; Figure S2). EDC4 is an established PB marker for mammalian cells and is important for PB formation[3f, 4b]. SGs were induced in HeLa cells by arsenite treatments and detected by fluorescent staining with anti-Ras GTPase-activating protein-binding protein 1 (G3BP1) antibody (75 μM arsenite, 30 min; Figure S3). G3BP1 foci have been used in previous IF studies to identify SGs in cells[3f]. See Supporting Methods for additional details of the PB and SG phenotypic screening workflow and data analysis.

SuTEx compounds were selected for phenotypic screening based on fragment-like size (median MW of 343 g/mol), physicochemical properties (hydrophobicity, polar surface area, prevalence of sp^3 centers) and LG diversity (1,2,3- and 1,2,4-triazoles; Figure S1 and Table S1). We also included SuTEx fragments with alkyl substituents (e.g., EKT158, AHL-006 and HHS-166), which can temper reactivity and improve stability[24]. We identified several compounds that reproducibly decreased the number of PBs per cell in compound treated, glucose-deprived cells (≥50% reduction in PBs/cell, 25 μM SuTEx fragment, 2 h; Figure 2 and S2). These PB inhibitors were enriched for 1,2,3-sulfonyl-triazoles containing alkyl- and aryl-substituents on both the adduct- and leaving-group (Figure 2 and S2). Several of these compounds showed a similar magnitude of PB blockade as the control compound and general protein translation inhibitor emetine[3f, 14b] (AHL-006, EKT231, and EKT132 vs emetine (50 nM, 2 h); Figure S2C). Intriguingly, treatment of cells with AMC-001 resulted in a statistically significant increase in PBs per glucose-deprived cell (>2-fold increase in PBs/cells with AMC-001 pretreatment, Figure 2 and S2B–C).

Next, we evaluated SuTEx compound effects on cellular SG levels to determine if this class of electrophiles can modulate different types of RNP granules (Figure S3). Several of the tested SuTEx compounds reduced cellular SG levels by >70% (EKT166, AHL-003) while other compounds displayed moderate, but statistically significant inhibitory activity (e.g., ~50% inhibition of SGs/cell by HHS-166, Figure 2 and S3B–D). When compared with PB modulators, we detected compounds that could block both types of RNP granules (AHL-003) as well as SuTEx ligands with enriched activity for PBs (EKT132) and SGs (EKT166, HHS-166; Figure 2 and S2–3). We also identified AHL-030 as an SG enhancer; treatment of cells with AHL-030 resulted in a ~2-fold increase in SGs per arsenite-treated cell (Figure 2 and S3C). Quantification and representative images from IF studies can be found in Table S2–3 and Figure S2–3.

In summary, our findings establish SuTEx ligands as a new class of electrophiles that can modulate cellular RNP granules in response to stress. The identification of distinct compounds for inhibiting or enhancing PBs and SGs in stressed cells should prove useful for functional investigation of these dynamic structures.

Features of protein sites liganded by SuTEx RNP granule modulators

An advantage of using covalent small molecules for ligand discovery is rapid target and binding site identifications using quantitative chemical proteomics. Target deconvolution represents an important, but often challenging, first step towards understanding mode of action for condensate-modifying compounds[11, 19]. The binding profiles obtained from chemical proteomics enable global selectivity profiling and bioinformatics-mediated discovery of enriched protein functions and domains underlying the PB- and SG-modulating activity of hit compounds.

We performed quantitative liquid-chromatography tandem mass spectrometry (LC-MS/MS) chemical proteomic studies to identify the target protein and binding site(s) of SuTEx fragments with RNP granule modulating activity. Inactive SuTEx compounds were also included as negative controls for direct comparison. SILAC light and heavy cells (HEK293T and HeLa) were treated with experimental conditions used for phenotypic screening including the SuTEx ligand pretreatment (25 μM, 2 h) followed by PB (glucose-deprivation, 15 min) and SG induction (75 μM arsenite, 30 min). Afterwards, cells were lysed, soluble proteomes treated with HHS-465 SuTEx probe (100 μM, 1 h), a global Tyr/Lys-reactive probe used previously for RNP granule investigations[23a], and samples processed to probe-modified peptides for LC-MS/MS analysis as previously reported[25], shown in Figure S4, and described in Supporting Methods.

We detected ~8,700 probe-modified sites (Tyr and Lys) in our aggregate HeLa and HEK293T chemical proteomic analyses. Organization of SG and PB modulators by hierarchical clustering of SILAC ratios (SR) of detected Tyr and Lys sites from SuTEx ligand competition of probe labeling revealed evidence of grouping based on active vs inactive hits for each respective RNP granule type (Figure 3A). We identified reproducibly liganded Tyr and Lys sites using the following criteria: 1) an average SILAC ratio (SR) > 2 across biological replicates, and 2) a SR > 2 in at least two biologically independent replicates. Using these criteria, a collection of 598 and 203 liganded sites (SR > 2) from compound-treated, stress-induced HeLa and HEK293T cells, respectively, emerged for further bioinformatic analysis. SuTEx electrophile reactivity in proteomes was comparable to hit rates (i.e., fragment-competed residues/total sites quantified) from ABPP screens of cysteine-directed electrophile libraries (~3–9% for SuTEx compared with ~4–7% for cysteine-directed electrophiles[26]). Interestingly, the median Tyr/Lys ratio for all liganded sites was ~0.8, which supports a moderate preference for lysine binding of SuTEx ligand hits (Figure S5). A complete list of liganded sites from chemoproteomic evaluation of SuTEx compounds can be found in Table S4–6.

Domain enrichment analyses of liganded sites identified statistically significant binding of SuTEx compounds at RBDs (KH, Helicase ATP-binding), ubiquitin-like, and YjeF N-terminal domains, which are reported to be involved in RNP granule regulation or

liquid–liquid phase separation (UBL[27], YjeF N-terminal[23a], KH domains[28]; Figure 3B and Table S7). Comparison of liganded proteins (311 proteins) to annotated RNP granule proteins[7b, 22b] revealed substantial overlap (118 proteins, ~38% overlap; Figure 3C). The remaining proteins without prior RNP granule annotation were enriched for functions involving cytoskeletal structures including intermediate filament proteins associated with the stress response and SG regulation[29] (Table S8). A comparison of liganded proteins against the Pharos database[30] showed differing levels of functional annotation and pharmacological tractability (Figure 3D). Gene Ontology (GO) analysis of liganded proteins identified protein folding along with structural, nucleotide, and energetic cellular processes as enriched functions that were also prominently observed in GO analyses of the RNP granule proteome (Figure 3E and F).

A more detailed evaluation of liganded RNP granule proteins[7b, 22b] identified SuTEx compounds targeting key protein families including chaperones (HSPB1, STIP1, calreticulin), nucleases (SND1, XRN2) and RNA-binding proteins (RBPs; PCBP1/2, HNRPK, hnRNPA/B). Several of these target proteins have demonstrated roles in phase separation (hnRNPA[1]) or maintenance of the liquid state of phase-separated droplets (e.g., HSPB1 maintenance of phase-separated, cytoplasmic TDP-43 droplets[31]). The liganded sites mapped to expected protein regions involved in RNP granule biology including RBDs (Y197 and K369 in the helicase domain of IF4A1; K23 in the KH domain of PCBP1) but also included domains mediating carbohydrate recognition (Y109 in the TNase-like domain of SND1) and dimerization (Y39 in the Phosphagen kinase N-terminal domain on KCRB; Table S6). Many of the liganded residues are sites for post-translational regulation including phosphorylation (IF4A1-Y197, SND1-Y109, KCRB-Y39) and ubiquitination/sumoylation (PCBP1-K23, IF4A1-K369, HSPB1-K123, PARK7-K130) as annotated by PhosphoSitePlus (HTP >10 or LTP >3 cutoffs). Importantly, we found ~12% of RNP granule proteins liganded by SuTEx SG/PB modulators were not targeted by cysteine-reactive fragment electrophiles evaluated in large-scale, cell-based screens[26b] (Table S9).

AHL-030 covalently binds the stress responsive EDC3 Y475 site

Next, we compared the collection of liganded sites with Tyr and Lys residues previously reported to couple stress response to RNP granule formation (i.e., RISKY sites[23a]; Figure 4A). We reasoned this comparison would facilitate prioritization of sites with prior annotation in the stress response of cells. From this list we identified a set of liganded RISKY sites that included the hyper-reactive tyrosine (Y475) on EDC3 that is a component of PBs involved in removal of the 7MG 5’ mRNA cap[2a, 4b, 7b]. The Y475 site is located in the YjeF_N domain, which has been reported to function in EDC3 self-dimerization[32] and recently annotated as a arsenite-sensitive site that regulates PB formation through regulation of EDC3 phosphorylation state and PPIs[23a].

Among the candidate PB-modulating SuTEx compounds, we focused on AHL-030 because of its PB-inhibitory, SG-enhancing activity in stressed cells and ability to ligand the EDC3 Y475 site (SR >2; Figure 4B–C and Table S6). Importantly, we identified a restricted number of reproducibly liganded sites (7 in total) in addition to EDC3 Y475 in chemoproteomic profiling studies of AHL-030 (Figure S6 and Table S6). We further

confirmed AHL-030 as an EDC3 ligand using competitive activity-based protein profiling (ABPP)[21]. Recombinant EDC3-expressing HEK293T cells were treated with a panel of RNP granule modulators including AHL-030 and the negative control compound EKT235 to evaluate structure-activity relationships (SAR, 25 μM compounds, 2 h). Cells were lysed and soluble proteomes labeled with HHS-465 (100 μM, 1 h, RT) followed by CuAAC with rhodamine-azide, SDS-PAGE and in-gel fluorescence scanning. By gel-based ABPP, we found that AHL-030 blocked HHS-465 probe labeling of EDC3 in a concentration-dependent manner as determined by reductions in fluorescent labeling of recombinant protein (IC_{50} = 6 μM, Figure 4D and E). Using the *in vitro* IC_{50}, we calculated the lipophilic efficiency (LipE) of AHL-030 to be ~7, which falls in the range of acceptable lipophilicity in relation to potency[33]. We showed the control compound (EKT235), additional PB (EKT231) and PB/SG modulators (AHL-003) were largely inactive against recombinant EDC3, which supports AHL-030 as a lead compound for future development of potent and selective EDC3-targeted ligands (Figure 4F).

Covalent binding of G3BP1 Y40 mediates the SG-modulating activity of HHS-166

RNP granule assembly and dissolution can be regulated through post-translational modifications[34] (PTMs). Protein phosphorylation, for example, regulates condensate formation through rapid and reversible modification of protein function, localization and interactions[35]. Reported examples include phosphorylation of the RNA-binding protein fused in sarcoma (FUS) and fragile X mental retardation protein (FMRP), which results in reduced[35a] and increased condensate formation[35c], respectively. We compared liganded sites from reported SG proteins with assigned PTMs from PhosphoSitePlus (HTP score ≥10 or LTP score ≥1; Table S10). We surmised this comparison would identify PTM sites that are amenable for developing targeted condensate-modulating compounds.

Our prioritization strategy identified key liganded PTM sites on SG proteins including G3BP1 (Y40[36], phosphorylation), HSPB1 (K123; acetylation, ubiquitination), and HNRPK (Y72[37], phosphorylation; Figure 5A and S7). A complete list of liganded PTM sites can be found in Table S10. The identification of G3BP1 was particularly interesting given its role as a nucleating protein for SGs and the identification of HHS-166 as a ligand for Y40 from our chemical proteomic studies (SR >2, Figure 5A–B and S8). Importantly, the SG-inhibitory activity of HHS-166 was demonstrated to be dose dependent (EC_{50} = 8 μM, LipE of ~3; Figure S9). The Y40 site is located in the nuclear transport factor 2 domain (NTF2) of G3BP1, which has been shown to be important for G3BP1 dimerization, a key event for SG formation *in vitro* and in cells[3a, b] (Figure 5C). Interestingly, G3BP1 Y40 was not detected by global phosphoproteomic analysis of condensates[35b] but was reported as a critical BTK-regulated phosphotyrosine for SG formation in response to viral infection[36].

To determine whether the cell biological effects mediated by HHS-166 were Y40-dependent, we expressed recombinant G3BP1 WT or Y40 mutant in previously established G3BP1/2 double knockout U20S (G3BP KO) cells[3a, 38] and evaluated the resulting effects on SG response to arsenite. We compared SG response of G3BP KO cells expressing a G3BP1 Y40 covalent binding- and phospho-deficient mutant (Y40F) with a phosphomimetic counterpart (Y40E). G3BP KO cells were previously shown to be deficient in arsenite-induced SG

formation[3a]. Expression of G3BP1 WT rescued this deficiency and restored cellular SG response to arsenite [1.6 vs 11 SGs/cell in (−)arsenite vs (+)arsenite, respectively; Figure 6A and B]. These G3BP1 WT-rescued cells responded to HHS-166 treatment, resulting in a statistically significant decrease in SGs (57% reduction in SGs/cell) that was not observed with pretreatment of a G3BP1 Y40- and SG-inactive compound (EKT231) or broad-reactive SuTEx probe (HHS-465, 9–13% reduction in SGs/cell for inactive compounds, respectively; Figure 6B). Notably, expression of G3BP1 Y40F resulted in cells that were deficient in arsenite-induced SG formation and insensitive to SuTEx compound treatments. Stress-induced SG formation of G3BP1 Y40E-rescued cells was comparable to WT counterpart but insensitive to HHS-166 treatment, demonstrating the importance of Y40 for SuTEx ligandability and SG inhibition (Figure 6A and B).

In summary, our studies identify G3BP1 Y40 as a key regulatory site for arsenite-induced SG formation and show that covalent modification of this residue by the SuTEx ligand HHS-166 inhibits SG assembly.

CONCLUSIONS

Aberrant condensate regulation is associated with a growing number of disease states (e.g., neurodegeneration, viral infection, cancer) and several therapeutic targets (TDP-43, FUS) are known to localize to these subcellular compartments[11]. Targeting disease-relevant condensates offers unique opportunities for therapeutic discovery but has so far proven challenging due to the compositional diversity and dynamic nature of these evolutionarily conserved structures[1, 39]. Here, we describe a covalent approach to discover condensate-modulating small molecules. The selection of SuTEx chemistry for our screening platform enabled access to ligandable Tyr/Lys residues, which are frequent in RNA-binding interfaces and can serve as sites for post-translational regulation, to perturb function of known RNP granule proteins as well as reveal new candidate targets proteome-wide.

We deployed a phenotypic screen for condensate-modulating small molecules by monitoring SG and PB formation in cells using established immunofluorescence markers[3f]. Our previous chemical proteomic studies identified sulfonyl-triazoles (SuTEx) as a cell-active electrophile for covalent targeting of RNA-binding and protein-protein interaction domains[22a], which are known to facilitate high valency interactions for assembly of condensed RNP networks[3a]. We pursued a fragment-based ligand discovery (FBLD) approach because of the ability to survey a larger fraction of chemical space with a smaller number of fragments[40]. SuTEx was chosen for FBLD because LG diversification with binding groups permitted integration of the sulfone into fragment design as opposed to appending this electrophile to existing ligands (e.g., using SuFEx[20a]).

Our screen identified SuTEx compounds that inhibited SGs (EKT166, HHS-166), PBs (EKT132), and both types of RNP granules in stressed cells (AHL-003; Figure 2 and S2–3). Unexpectedly, we also identified SuTEx ligands that enhanced stress-induced RNP granule levels in compound-treated cells. Pretreatment of cells with AMC-001 resulted in a statistically significant increase in PBs of glucose-deprived cells (>200% increase; Figure 2 and S2). These effects appeared specific for PBs as analogous pretreatments in

arsenite-stressed cells resulted in negligible effects on the number of SGs per cell (Figure S3).

We performed competitive LC-MS/MS ABPP studies to establish covalent binding profiles for active SuTEx compound hits. The outcome of these studies established, to the best of our knowledge, the first comprehensive map directly connecting RNP granule modulating activity with protein sites engaged by bioactive compounds in cells. In aggregate, we quantified >770 Tyr and Lys sites that are ligandable for developing covalent binders with RNP granule-modulating activity in cells. The proteomic reactivity of SuTEx electrophiles in cells (~3–9%) was comparable to hit rates previously reported for screening electrophile libraries[26] (Figure 3).

Among the list of liganded RNP-granule proteins, we identified key RBPs (hnRNPA) and chaperone proteins (HSPB1) that have demonstrated roles in phase separation[1] or maintenance of condensates[31]. The liganded sites mapped to functional domains of proteins that are reported sites for post-translational phosphorylation, ubiquitination, and sumoylation (Table S6–8 and S10). By expanding the ligandable RNP granule proteome, the pharmacological tractability of individual proteins and sites within functional domains can be further explored to develop condensate-modulating compounds in future studies. Importantly, a subset of RNP granule proteins liganded by SuTEx fragments (~12%, Table S9) were not detected in cell-based screens of large electrophile libraries of cysteine-reactive compounds (280+ members[26b]). These findings highlight the need for Tyr/Lys-targeting chemistry for accessing RNP granule proteins that can be difficult to target with cysteine-reactive electrophiles.

Compared with previous Tyr-directed FBLD reports using 1,2,4-SuTEx compounds[24], the current study identified a moderate preference for Lys compared with Tyr binding among the 1,2,3-SuTEx fragment hits (Y/K ratio of ~0.8, Figure S5). This finding was important because it positions the largely underexplored 1,2,3-triazole LG as a feasible starting point for advancing SuTEx chemistry towards development of Lys-targeted ligands. The increased frequency of Lys among the liganded sites of SG/PB modulators was perhaps not surprising given that protein-RNA interfaces are abundant with Tyr and Lys residues and typically enriched for the latter to presumably mediate RNA phosphate recognition[12]. Thus, LG selection is an important criterion for guiding the future expansion of sulfone-based electrophile libraries to fully assess opportunities for chemical biology of RNP granules.

We demonstrated the utility of our integrated phenotypic screening and chemoproteomic approach through follow-up studies on compounds that affected dimerization domains of known RNP granule proteins. We identified AHL-030 as a unique hit compound because of its opposing activity to enhance SGs while modestly inhibiting PBs in stressed cells (Figure 2). Competitive ABPP studies localized AHL-030 site of binding to Y475 in the YjeF_N domain of EDC3, which has been reported to function in self-dimerization[32] and mediate PB response to stress[23a] (Figure 4). While additional studies are needed to understand AHL-030 mode of action, we demonstrated concentration-dependent binding to recombinant EDC3 that was specific for AHL-030 compared with other PB (EKT231) and PB/SG (AHL-003) modulators identified (Figure 4D–F).

We provide evidence in support of site-specific activity for the SG-modulating compound HHS-166. This compound showed dose-dependent inhibition of arsenite-induced SG formation, and liganded G3BP1 Y40 in the NTF2 dimerization domain of this essential nucleating protein for SG regulation[3a, b] (Figure 5 and S9). The SG modulating activity of HHS-166 was lost when covalent binding-deficient mutants (Y40E or Y40F) of G3BP1 were expressed in G3BP KO cells (Figure 6). Further, the phosphodeficient Y40F G3BP1 mutant was impaired in arsenite-induced SG formation indicating that the Y40 phosphosite is a general regulatory site for both viral[36] and oxidative stress response of cells (Figure 6).

There are a few limitations in our study that can be addressed in future studies. Our conclusions rely on counting RNP granules that are detectable by IF microscopy. There is some evidence that RNP granules exert cellular effects at sizes that do not provide a measurable optical phenotype. Additionally, the presence of microscopically visible RNP granules may depend on the IF protein marker utilized. In our studies, we selected G3BP1 and EDC4 – both of which have been shown to be critical for RNP granule formation[3f] – as biomarkers of SG and PB structures, respectively. The inclusion of additional functional markers could further refine the evaluation of compositionally distinct RNP granules. We chose arsenite and glucose deprivation to induce RNP granules because these are widely adopted model systems[3f] but additional experimental conditions that capture disease-relevant condensate biology should be explored in future studies[1]. Our cellular screening conditions (25 μM SuTEx ligand treatment for 2 h) were chosen based on previous SuTEx compound screens in cells[41] that also matched conditions reported for cell-based screens of cysteine-reactive fragment electrophile libraries[26b]. Future screening efforts using SuTEx libraries, and fragment electrophiles in general, should identify appropriate compound concentrations and treatment times to address off-target activity and stability of reactive molecules in biological systems. Future work could also evaluate whether SuTEx chemoproteomics can be deployed for functional profiling of condensates found in different subcellular locations including the plasma membrane and nucleus[1].

In summary, we present a systematic approach for discovering condensate-modulating covalent small molecules with defined protein interaction profiles to serve as chemical probes for investigating biomolecular condensate regulation and pharmacological tractability.

Supplementary Material

Refer to Web version on PubMed Central for supplementary material.

ACKNOWLEDGMENTS

We thank Mark Ross and all members of the Hsu Lab for helpful discussions and review of the manuscript. This work was supported by the National Institutes of Health Grants (DA043571 and GM144472 to K.-L.H.; CA009109 to A.L.B.; GM132189 to R.E.K), University of Virginia Cancer Center (NCI Cancer Center Support Grant No. 5P30CA044579-27 to K.-L.H.), the Robbins Family MRA Young Investigator Award from the Melanoma Research Alliance (http://doi.org/10.48050/pc.gr.80540 to K.-L.H.), the Mark Foundation for Cancer Research (Emerging Leader Award to K.-L.H.), and a Recruitment of Rising Stars Award from CPRIT (RR220063 to K.-L.H.). K.W.S. and R.E.K. thank Princeton University for financial support. We acknowledge the Keck Center for Cellular Imaging for the usage of the Leica SP5X microscopy system (PI:AP, NIH-RR025616). We thank Jeffrey Brulet and Kun Yuan for assistance in synthesis of SuTEx compounds and probes. We thank Heung-Sik Hahm and Emmanuel

Toroitich for general help with the SuTEx project. A special thanks to Timothy B. Ware for helping to blind the microscopy slides. We thank D.W. Sanders and C. Brangwynne for providing the G3BP1/2 KO cell line.

REFERENCES

(1). Banani SF; Lee HO; Hyman AA; Rosen MK Biomolecular condensates: organizers of cellular biochemistry. Nat Rev Mol Cell Biol 2017, 18 (5), 285–298. DOI: 10.1038/nrm.2017.7. [PubMed: 28225081]

(2) (a). Ivanov P; Kedersha N; Anderson P Stress Granules and Processing Bodies in Translational Control. Cold Spring Harb Perspect Biol 2019, 11 (5). DOI: 10.1101/cshperspect.a032813. (b)Shin Y; Brangwynne CP Liquid phase condensation in cell physiology and disease. Science 2017, 357 (6357). DOI: 10.1126/science.aaf4382.

(3) (a). Sanders DW; Kedersha N; Lee DSW; Strom AR; Drake V; Riback JA; Bracha D; Eeftens JM; Iwanicki A; Wang A; et al. Competing Protein-RNA Interaction Networks Control Multiphase Intracellular Organization. Cell 2020, 181 (2), 306–324 e328. DOI: 10.1016/j.cell.2020.03.050. [PubMed: 32302570] (b)Yang P; Mathieu C; Kolaitis RM; Zhang P; Messing J; Yurtsever U; Yang Z; Wu J; Li Y; Pan Q; et al. G3BP1 Is a Tunable Switch that Triggers Phase Separation to Assemble Stress Granules. Cell 2020, 181 (2), 325–345 e328. DOI: 10.1016/j.cell.2020.03.046. [PubMed: 32302571] (c)Sheth U; Parker R Decapping and decay of messenger RNA occur in cytoplasmic processing bodies. Science 2003, 300 (5620), 805–808. DOI: 10.1126/science.1082320. [PubMed: 12730603] (d)Collier NC; Schlesinger MJ The dynamic state of heat shock proteins in chicken embryo fibroblasts. J Cell Biol 1986, 103 (4), 1495–1507. DOI: 10.1083/jcb.103.4.1495. [PubMed: 3533955] (e)Nover L; Scharf KD; Neumann D Cytoplasmic heat shock granules are formed from precursor particles and are associated with a specific set of mRNAs. Mol Cell Biol 1989, 9 (3), 1298–1308. DOI: 10.1128/mcb.9.3.1298-1308.1989. [PubMed: 2725500] (f)Kedersha N; Anderson P Mammalian Stress Granules and Processing Bodies. In Translation Initiation: Cell Biology, High-Throughput Methods, and Chemical-Based Approaches, Methods in Enzymology, 2007; pp 61–81.

(4) (a). Standart N; Weil D P-Bodies: Cytosolic Droplets for Coordinated mRNA Storage. Trends Genet 2018, 34 (8), 612–626. DOI: 10.1016/j.tig.2018.05.005. [PubMed: 29908710] (b)Luo Y; Na Z; Slavoff SA P-Bodies: Composition, Properties, and Functions. Biochemistry 2018, 57 (17), 2424–2431. DOI: 10.1021/acs.biochem.7b01162. [PubMed: 29381060]

(5) (a). Riggs CL; Kedersha N; Ivanov P; Anderson P Mammalian stress granules and P bodies at a glance. J Cell Sci 2020, 133 (16). DOI: 10.1242/jcs.242487.(b)Protter DSW; Parker R Principles and Properties of Stress Granules. Trends Cell Biol 2016, 26 (9), 668–679. DOI: 10.1016/j.tcb.2016.05.004. [PubMed: 27289443]

(6) (a). Guillen-Boixet J; Kopach A; Holehouse AS; Wittmann S; Jahnel M; Schlussler R; Kim K; Trussina I; Wang J; Mateju D; et al. RNA-Induced Conformational Switching and Clustering of G3BP Drive Stress Granule Assembly by Condensation. Cell 2020, 181 (2), 346–361 e317. DOI: 10.1016/j.cell.2020.03.049. [PubMed: 32302572] (b)Decker CJ; Parker R P-bodies and stress granules: possible roles in the control of translation and mRNA degradation. Cold Spring Harb Perspect Biol 2012, 4 (9), a012286. DOI: 10.1101/cshperspect.a012286. [PubMed: 22763747] (c)Stoecklin G; Kedersha N Relationship of GW/P-bodies with stress granules. Adv Exp Med Biol 2013, 768, 197–211. DOI: 10.1007/978-1-4614-5107-5_12. [PubMed: 23224972]

(7) (a). Lavalee M; Curdy N; Laurent C; Fournie JJ; Franchini DM Cancer cell adaptability: turning ribonucleoprotein granules into targets. Trends Cancer 2021, 7 (10), 902–915. DOI: 10.1016/j.trecan.2021.05.006. [PubMed: 34144941] (b)Hubstenberger A; Courel M; Benard M; Souquere S; Ernoult-Lange M; Chouaib R; Yi Z; Morlot JB; Munier A; Fradet M; et al. P-Body Purification Reveals the Condensation of Repressed mRNA Regulons. Mol Cell 2017, 68 (1), 144–157 e145. DOI: 10.1016/j.molcel.2017.09.003. [PubMed: 28965817] (c)Brengues M; Teixeira D; Parker R Movement of eukaryotic mRNAs between polysomes and cytoplasmic processing bodies. Science 2005, 310 (5747), 486–489. DOI: 10.1126/science.1115791. [PubMed: 16141371]

(8) (a). Baradaran-Heravi Y; Van Broeckhoven C; van der Zee J Stress granule mediated protein aggregation and underlying gene defects in the FTD-ALS spectrum. Neurobiol Dis 2020, 134, 104639. DOI: 10.1016/j.nbd.2019.104639. [PubMed: 31626953] (b)Hans F; Glasebach

H; Kahle PJ Multiple distinct pathways lead to hyperubiquitylated insoluble TDP-43 protein independent of its translocation into stress granules. J Biol Chem 2020, 295 (3), 673–689. DOI: 10.1074/jbc.RA119.010617. [PubMed: 31780563] (c)Mackenzie IR; Nicholson AM; Sarkar M; Messing J; Purice MD; Pottier C; Annu K; Baker M; Perkerson RB; Kurti A; et al. TIA1 Mutations in Amyotrophic Lateral Sclerosis and Frontotemporal Dementia Promote Phase Separation and Alter Stress Granule Dynamics. Neuron 2017, 95 (4), 808–816 e809. DOI: 10.1016/j.neuron.2017.07.025. [PubMed: 28817800] (d)Marmor-Kollet H; Siany A; Kedersha N; Knafo N; Rivkin N; Danino YM; Moens TG; Olender T; Sheban D; Cohen N; et al. Spatiotemporal Proteomic Analysis of Stress Granule Disassembly Using APEX Reveals Regulation by SUMOylation and Links to ALS Pathogenesis. Mol Cell 2020, 80 (5), 876–891 e876. DOI: 10.1016/j.molcel.2020.10.032. [PubMed: 33217318] (e)Reineke LC; Lloyd RE The stress granule protein G3BP1 recruits protein kinase R to promote multiple innate immune antiviral responses. J Virol 2015, 89 (5), 2575–2589. DOI: 10.1128/JVI.02791-14. [PubMed: 25520508] (f)Anderson P; Kedersha N; Ivanov P Stress granules, P-bodies and cancer. Biochim Biophys Acta 2015, 1849 (7), 861–870. DOI: 10.1016/j.bbagrm.2014.11.009. [PubMed: 25482014] (g)Gordon DE; Jang GM; Bouhaddou M; Xu J; Obernier K; O'Meara MJ; Guo JZ; Swaney DL; Tummino TA; Huttenhain R; et al. A SARS-CoV-2-Human Protein-Protein Interaction Map Reveals Drug Targets and Potential Drug-Repurposing. bioRxiv 2020. DOI: 10.1101/2020.03.22.002386.(h)Cui Q; Bi H; Lv Z; Wu Q; Hua J; Gu B; Huo C; Tang M; Chen Y; Chen C; et al. Diverse CMT2 neuropathies are linked to aberrant G3BP interactions in stress granules. Cell 2023. DOI: 10.1016/j.cell.2022.12.046.

(9) (a). Kwon S; Zhang Y; Matthias P The deacetylase HDAC6 is a novel critical component of stress granules involved in the stress response. Genes Dev 2007, 21 (24), 3381–3394. DOI: 10.1101/gad.461107. [PubMed: 18079183] (b)Arimoto K; Fukuda H; Imajoh-Ohmi S; Saito H; Takekawa M Formation of stress granules inhibits apoptosis by suppressing stress-responsive MAPK pathways. Nat Cell Biol 2008, 10 (11), 1324–1332. DOI: 10.1038/ncb1791. [PubMed: 18836437] (c)Fujimura K; Sasaki AT; Anderson P Selenite targets eIF4E-binding protein-1 to inhibit translation initiation and induce the assembly of non-canonical stress granules. Nucleic Acids Res 2012, 40 (16), 8099–8110. DOI: 10.1093/nar/gks566. [PubMed: 22718973] (d)Fournier MJ; Gareau C; Mazroui R The chemotherapeutic agent bortezomib induces the formation of stress granules. Cancer Cell Int 2010, 10, 12. DOI: 10.1186/1475-2867-10-12. [PubMed: 20429927] (e)Kaehler C; Isensee J; Hucho T; Lehrach H; Krobitsch S 5-Fluorouracil affects assembly of stress granules based on RNA incorporation. Nucleic Acids Res 2014, 42 (10), 6436–6447. DOI: 10.1093/nar/gku264. [PubMed: 24728989]

(10). Hallacli E; Kayatekin C; Nazeen S; Wang XH; Sheinkopf Z; Sathyakumar S; Sarkar S; Jiang X; Dong X; Di Maio R; et al. The Parkinson's disease protein alpha-synuclein is a modulator of processing bodies and mRNA stability. Cell 2022, 185 (12), 2035–2056 e2033. DOI: 10.1016/j.cell.2022.05.008. [PubMed: 35688132]

(11). Mitrea DM; Mittasch M; Gomes BF; Klein IA; Murcko MA Modulating biomolecular condensates: a novel approach to drug discovery. Nat Rev Drug Discov 2022, 21 (11), 841–862. DOI: 10.1038/s41573-022-00505-4. [PubMed: 35974095]

(12). Kruger DM; Neubacher S; Grossmann TN Protein-RNA interactions: structural characteristics and hotspot amino acids. RNA 2018, 24 (11), 1457–1465. DOI: 10.1261/rna.066464.118. [PubMed: 30093489]

(13). Hentze MW; Castello A; Schwarzl T; Preiss T A brave new world of RNA-binding proteins. Nat Rev Mol Cell Biol 2018, 19 (5), 327–341. DOI: 10.1038/nrm.2017.130. [PubMed: 29339797]

(14) (a). Cougot N; Babajko S; Seraphin B Cytoplasmic foci are sites of mRNA decay in human cells. J Cell Biol 2004, 165 (1), 31–40. DOI: 10.1083/jcb.200309008. [PubMed: 15067023] (b)Colombrita C; Zennaro E; Fallini C; Weber M; Sommacal A; Buratti E; Silani V; Ratti A TDP-43 is recruited to stress granules in conditions of oxidative insult. J Neurochem 2009, 111 (4), 1051–1061. DOI: 10.1111/j.1471-4159.2009.06383.x. [PubMed: 19765185]

(15) (a). Bordeleau ME; Matthews J; Wojnar JM; Lindqvist L; Novac O; Jankowsky E; Sonenberg N; Northcote P; Teesdale-Spittle P; Pelletier J Stimulation of mammalian translation initiation factor eIF4A activity by a small molecule inhibitor of eukaryotic translation. Proc Natl Acad Sci U S A 2005, 102 (30), 10460–10465. DOI: 10.1073/pnas.0504249102. [PubMed: 16030146] (b)Low WK; Dang Y; Schneider-Poetsch T; Shi Z; Choi NS; Merrick WC; Romo D; Liu JO Inhibition

of eukaryotic translation initiation by the marine natural product pateamine A. Mol Cell 2005, 20 (5), 709–722. DOI: 10.1016/j.molcel.2005.10.008. [PubMed: 16337595] (c)Bordeleau ME; Mori A; Oberer M; Lindqvist L; Chard LS; Higa T; Belsham GJ; Wagner G; Tanaka J; Pelletier J Functional characterization of IRESes by an inhibitor of the RNA helicase eIF4A. Nat Chem Biol 2006, 2 (4), 213–220. DOI: 10.1038/nchembio776. [PubMed: 16532013]

(16) (a). Ayache J; Benard M; Ernoult-Lange M; Minshall N; Standart N; Kress M; Weil D P-body assembly requires DDX6 repression complexes rather than decay or Ataxin2/2L complexes. Mol Biol Cell 2015, 26 (14), 2579–2595. DOI: 10.1091/mbc.E15-03-0136. [PubMed: 25995375] (b)Aizer A; Brody Y; Ler LW; Sonenberg N; Singer RH; Shav-Tal Y The dynamics of mammalian P body transport, assembly, and disassembly in vivo. Mol Biol Cell 2008, 19 (10), 4154–4166. DOI: 10.1091/mbc.E08-05-0513. [PubMed: 18653466]

(17) (a). Fang MY; Markmiller S; Vu AQ; Javaherian A; Dowdle WE; Jolivet P; Bushway PJ; Castello NA; Baral A; Chan MY; et al. Small-Molecule Modulation of TDP-43 Recruitment to Stress Granules Prevents Persistent TDP-43 Accumulation in ALS/FTD. Neuron 2019, 103 (5), 802–819 e811. DOI: 10.1016/j.neuron.2019.05.048. [PubMed: 31272829] (b)Sreedharan J; Blair IP; Tripathi VB; Hu X; Vance C; Rogelj B; Ackerley S; Durnall JC; Williams KL; Buratti E; et al. TDP-43 mutations in familial and sporadic amyotrophic lateral sclerosis. Science 2008, 319 (5870), 1668–1672. DOI: 10.1126/science.1154584. [PubMed: 18309045]

(18). Cai H; Liu X; Zhang F; Han QY; Liu ZS; Xue W; Guo ZL; Zhao JM; Sun LM; Wang N; et al. G3BP1 Inhibition Alleviates Intracellular Nucleic Acid-Induced Autoimmune Responses. J Immunol 2021, 206 (10), 2453–2467. DOI: 10.4049/jimmunol.2001111. [PubMed: 33941659]

(19). Patel A; Mitrea D; Namasivayam V; Murcko MA; Wagner M; Klein IA Principles and functions of condensate modifying drugs. Frontiers in Molecular Biosciences 2022, 9, Review. DOI: 10.3389/fmolb.2022.1007744.

(20) (a). Dong J; Krasnova L; Finn MG; Sharpless KB Sulfur(VI) fluoride exchange (SuFEx): another good reaction for click chemistry. Angew Chem Int Ed Engl 2014, 53 (36), 9430–9448. DOI: 10.1002/anie.201309399. [PubMed: 25112519] (b)Jones LH; Kelly JW Structure-based design and analysis of SuFEx chemical probes. RSC Med Chem 2020, 11 (1), 10–17. DOI: 10.1039/c9md00542k. [PubMed: 33479601]

(21). Grams RJ; Hsu KL Reactive chemistry for covalent probe and therapeutic development. Trends Pharmacol Sci 2022, 43 (3), 249–262. DOI: 10.1016/j.tips.2021.12.002. [PubMed: 34998611]

(22) (a). Hahm HS; Toroitich EK; Borne AL; Brulet JW; Libby AH; Yuan K; Ware TB; McCloud RL; Ciancone AM; Hsu KL Global targeting of functional tyrosines using sulfur-triazole exchange chemistry. Nat Chem Biol 2020, 16 (2), 150–159. DOI: 10.1038/s41589-019-0404-5. [PubMed: 31768034] (b)Youn JY; Dyakov BJA; Zhang J; Knight JDR; Vernon RM; Forman-Kay JD; Gingras AC Properties of Stress Granule and P-Body Proteomes. Mol Cell 2019, 76 (2), 286–294. DOI: 10.1016/j.molcel.2019.09.014. [PubMed: 31626750]

(23) (a). Ciancone AM; Hosseinibarkooie S; Bai DL; Borne AL; Ferris HA; Hsu KL Global profiling identifies a stress-responsive tyrosine site on EDC3 regulating biomolecular condensate formation. Cell Chem Biol 2022, 29 (12), 1709–1720 e1707. DOI: 10.1016/j.chembiol.2022.11.008. [PubMed: 36476517] (b)Markmiller S; Soltanieh S; Server KL; Mak R; Jin W; Fang MY; Luo EC; Krach F; Yang D; Sen A; et al. Context-Dependent and Disease-Specific Diversity in Protein Interactions within Stress Granules. Cell 2018, 172 (3), 590–604 e513. DOI: 10.1016/j.cell.2017.12.032. [PubMed: 29373831]

(24). Brulet JW; Borne AL; Yuan K; Libby AH; Hsu KL Liganding Functional Tyrosine Sites on Proteins Using Sulfur-Triazole Exchange Chemistry. J Am Chem Soc 2020, 142 (18), 8270–8280. DOI: 10.1021/jacs.0c00648. [PubMed: 32329615]

(25). Huang T; Hosseinibarkooie S; Borne AL; Granade ME; Brulet JW; Harris TE; Ferris HA; Hsu K-L Chemoproteomic profiling of kinases in live cells using electrophilic sulfonyl triazole probes. Chemical Science 2021, 12 (9), 3295–3307, 10.1039/D0SC06623K. DOI: 10.1039/d0sc06623k. [PubMed: 34164099]

(26) (a). Backus KM; Correia BE; Lum KM; Forli S; Horning BD; Gonzalez-Paez GE; Chatterjee S; Lanning BR; Teijaro JR; Olson AJ; et al. Proteome-wide covalent ligand discovery in native biological systems. Nature 2016, 534 (7608), 570–574. DOI: 10.1038/nature18002. [PubMed: 27309814] (b)Kuljanin M; Mitchell DC; Schweppe DK; Gikandi AS; Nusinow DP; Bulloch

NJ; Vinogradova EV; Wilson DL; Kool ET; Mancias JD; et al. Reimagining high-throughput profiling of reactive cysteines for cell-based screening of large electrophile libraries. Nat Biotechnol 2021, 39 (5), 630–641. DOI: 10.1038/s41587-020-00778-3. [PubMed: 33398154]

(27). Zheng T; Galagedera SKK; Castaneda CA Previously uncharacterized interactions between the folded and intrinsically disordered domains impart asymmetric effects on UBQLN2 phase separation. Protein Sci 2021, 30 (7), 1467–1481. DOI: 10.1002/pro.4128. [PubMed: 34029402]

(28). Nielsen FC; Nielsen J; Kristensen MA; Koch G; Christiansen J Cytoplasmic trafficking of IGF-II mRNA-binding protein by conserved KH domains. J Cell Sci 2002, 115 (Pt 10), 2087–2097. DOI: 10.1242/jcs.115.10.2087. [PubMed: 11973350]

(29) (a). Pattabiraman S; Azad GK; Amen T; Brielle S; Park JE; Sze SK; Meshorer E; Kaganovich D Vimentin protects differentiating stem cells from stress. Sci Rep 2020, 10 (1), 19525. DOI: 10.1038/s41598-020-76076-4. [PubMed: 33177544] (b)Toivola DM; Strnad P; Habtezion A; Omary MB Intermediate filaments take the heat as stress proteins. Trends Cell Biol 2010, 20 (2), 79–91. DOI: 10.1016/j.tcb.2009.11.004. [PubMed: 20045331]

(30). Sheils TK; Mathias SL; Kelleher KJ; Siramshetty VB; Nguyen DT; Bologa CG; Jensen LJ; Vidovic D; Koleti A; Schurer SC; et al. TCRD and Pharos 2021: mining the human proteome for disease biology. Nucleic Acids Res 2021, 49 (D1), D1334–D1346. DOI: 10.1093/nar/gkaa993. [PubMed: 33156327]

(31). Lu S; Hu J; Arogundade OA; Goginashvili A; Vazquez-Sanchez S; Diedrich JK; Gu J; Blum J; Oung S; Ye Q; et al. Heat-shock chaperone HSPB1 regulates cytoplasmic TDP-43 phase separation and liquid-to-gel transition. Nat Cell Biol 2022, 24 (9), 1378–1393. DOI: 10.1038/s41556-022-00988-8. [PubMed: 36075972]

(32). Ling SH; Decker CJ; Walsh MA; She M; Parker R; Song H Crystal structure of human Edc3 and its functional implications. Mol Cell Biol 2008, 28 (19), 5965–5976. DOI: 10.1128/MCB.00761-08. [PubMed: 18678652]

(33). Leeson PD; Springthorpe B The influence of drug-like concepts on decision-making in medicinal chemistry. Nat Rev Drug Discov 2007, 6 (11), 881–890. DOI: 10.1038/nrd2445. [PubMed: 17971784]

(34). Hofweber M; Dormann D Friend or foe-Post-translational modifications as regulators of phase separation and RNP granule dynamics. J Biol Chem 2019, 294 (18), 7137–7150. DOI: 10.1074/jbc.TM118.001189. [PubMed: 30587571]

(35) (a). Monahan Z; Ryan VH; Janke AM; Burke KA; Rhoads SN; Zerze GH; O'Meally R; Dignon GL; Conicella AE; Zheng W; et al. Phosphorylation of the FUS low-complexity domain disrupts phase separation, aggregation, and toxicity. EMBO J 2017, 36 (20), 2951–2967. DOI: 10.15252/embj.201696394. [PubMed: 28790177] (b)Sridharan S; Hernandez-Armendariz A; Kurzawa N; Potel CM; Memon D; Beltrao P; Bantscheff M; Huber W; Cuylen-Haering S; Savitski MM Systematic discovery of biomolecular condensate-specific protein phosphorylation. Nat Chem Biol 2022, 18 (10), 1104–1114. DOI: 10.1038/s41589-022-01062-y. [PubMed: 35864335] (c)Tsang B; Arsenault J; Vernon RM; Lin H; Sonenberg N; Wang LY; Bah A; Forman-Kay JD Phosphoregulated FMRP phase separation models activity-dependent translation through bidirectional control of mRNA granule formation. Proc Natl Acad Sci U S A 2019, 116 (10), 4218–4227. DOI: 10.1073/pnas.1814385116. [PubMed: 30765518]

(36). S, S. YK; Sim DCN; Carissimo G; Lim HH; Lam KP Bruton's Tyrosine Kinase phosphorylates scaffolding and RNA-binding protein G3BP1 to induce stress granule aggregation during host sensing of foreign ribonucleic acids. J Biol Chem 2022, 102231. DOI: 10.1016/j.jbc.2022.102231. [PubMed: 35798143]

(37). Kim HJ; Lee JJ; Cho JH; Jeong J; Park AY; Kang W; Lee KJ Heterogeneous nuclear ribonucleoprotein K inhibits heat shock-induced transcriptional activity of heat shock factor 1. J Biol Chem 2017, 292 (31), 12801–12812. DOI: 10.1074/jbc.M117.774992. [PubMed: 28592492]

(38). Kedersha N; Panas MD; Achorn CA; Lyons S; Tisdale S; Hickman T; Thomas M; Lieberman J; McInerney GM; Ivanov P; et al. G3BP-Caprin1-USP10 complexes mediate stress granule condensation and associate with 40S subunits. J Cell Biol 2016, 212 (7), 845–860. DOI: 10.1083/jcb.201508028. [PubMed: 27022092]

(39). Conti BA; Oppikofer M Biomolecular condensates: new opportunities for drug discovery and RNA therapeutics. Trends Pharmacol Sci 2022, 43 (10), 820–837. DOI: 10.1016/j.tips.2022.07.001. [PubMed: 36028355]

(40). Erlanson DA; Fesik SW; Hubbard RE; Jahnke W; Jhoti H Twenty years on: the impact of fragments on drug discovery. Nat Rev Drug Discov 2016, 15 (9), 605–619. DOI: 10.1038/nrd.2016.109. [PubMed: 27417849]

(41). Toroitich EK; Ciancone AM; Hahm HS; Brodowski SM; Libby AH; Hsu KL Discovery of a Cell-Active SuTEx Ligand of Prostaglandin Reductase 2. Chembiochem 2021, 22 (12), 2134–2139. DOI: 10.1002/cbic.202000879. [PubMed: 33861519]

(42). Mi H; Muruganujan A; Casagrande JT; Thomas PD Large-scale gene function analysis with the PANTHER classification system. Nat Protoc 2013, 8 (8), 1551–1566. DOI: 10.1038/nprot.2013.092. [PubMed: 23868073]

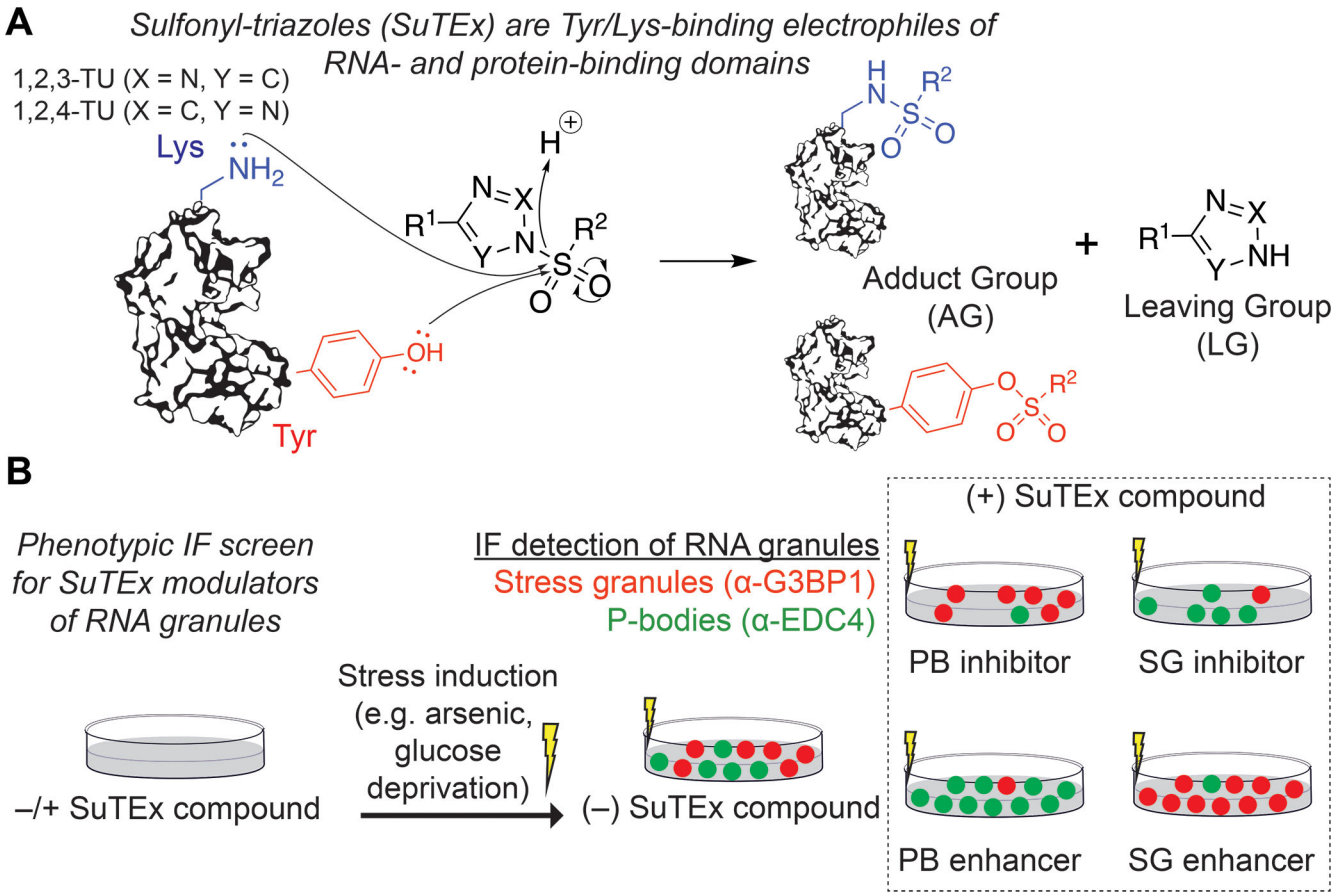

Figure 1. Phenotypic screening for condensate-modulating SuTEx electrophiles.

(A) Sulfonyl-triazoles are Tyr/Lys-reactive electrophiles with activity enriched for covalent binding to RNA-binding (RBD) and protein-protein interaction (PPI) domains via sulfur-triazole exchange (SuTEx) chemistry. (B) Phenotypic screening by immunofluorescence (IF) to identify SuTEx electrophile compounds that can function as PB and/or SG inhibitors or enhancers. SuTEx ligand-protein interactions of condensate-modulating compounds are deconvoluted by quantitative chemical proteomics.

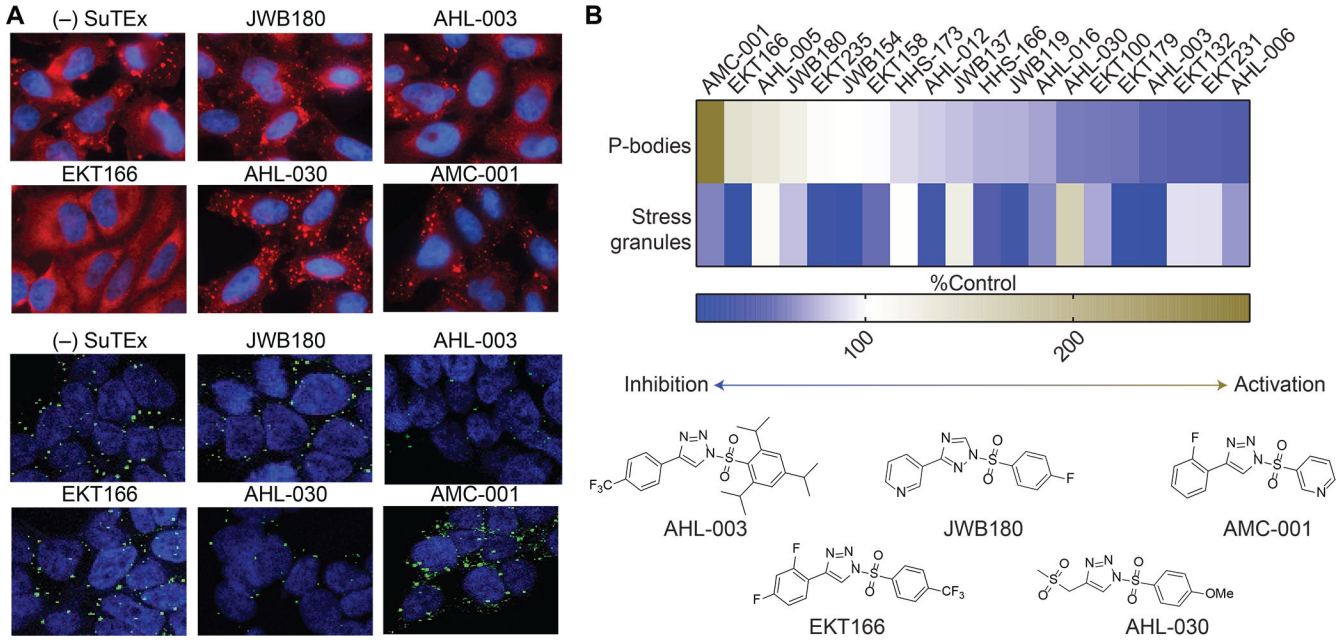

Figure 2. SuTEx electrophiles function as different classes of PB and SG modulators.

(A) Representative immunofluorescence images depicting effects of SuTEx compound treatments on stress granules (α-G3BP1, red) and P-bodies (α-EDC4, green) in arsenite-treated HeLa and glucose-deprived HEK293T cells, respectively. No treatment [(−)SuTEx] or treatment with a negative control SuTEx compound (JWB180) results in negligible effects on RNP granules in stressed cells. Data are representative of $n = 2–3$ biologically independent replicates. (B) Heat map for P-bodies and stress granules as a percentage of control for the complete SuTEx compound library screened. Heatmap is sorted by PBs. Data are representative of $n = 2–3$ biologically independent replicates. Chemical structures of lead SuTEx hit molecules are shown.

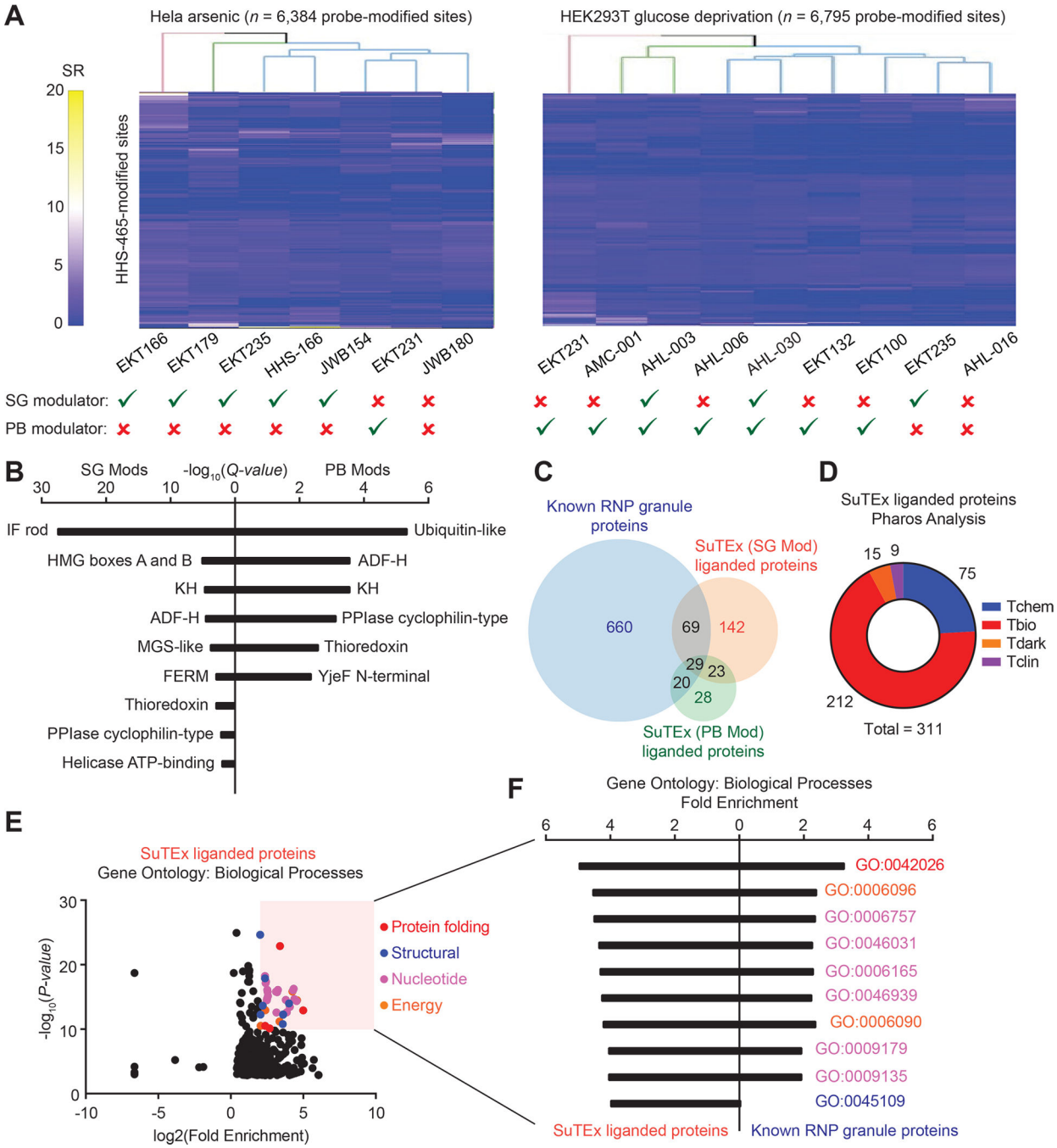

Figure 3. Expanding the ligandable proteome for RNP granule modulation.

(A) Heat map depicting Tyr- and Lys-probe-modified sites detected by LC-MS/MS sorted by compound (columns, named below) and hierarchically clustered based on competition ratios (high SR = greater competition) for each probe-modified site (rows). Heat maps are separated by SG-modulators in arsenite-treated HeLa cells (left) and PB-modulators in glucose-deprived HEK293T cells (right). Data are representative of $n = 2–5$ biologically independent replicates. (B) Domain enrichment analysis[22a] of liganded sites (SR >2) for SG- (left) and PB-modulating (right) SuTEx compounds. (C) Venn diagram comparing liganded

proteins (SR >2) in stressed cells with the reported RNP granule proteome. See Supporting Tables for the complete list of proteins used for comparison. (D) Target development level of liganded proteins based on the Pharos database[30]. (E) Plot of fold-enrichment ('FE', x-axis, log2-scale) as a function of *P*-value (y-axis, −log10-scale) for Gene Ontology (GO) enrichment analysis (PANTHER[42]) for biological processes overrepresented in liganded proteins from stressed cells. Significantly changed GO terms are highlighted (red box, log2 (FE) > 2 and $-\log_{10}$(*P*-value) > 10). (F) Top 10 GO terms by FE for SuTEx liganded proteins compared with GO analysis of the RNP granule proteome. Several GO terms were found to be enriched for both SuTEx liganded- and reported RNP granule-proteins.

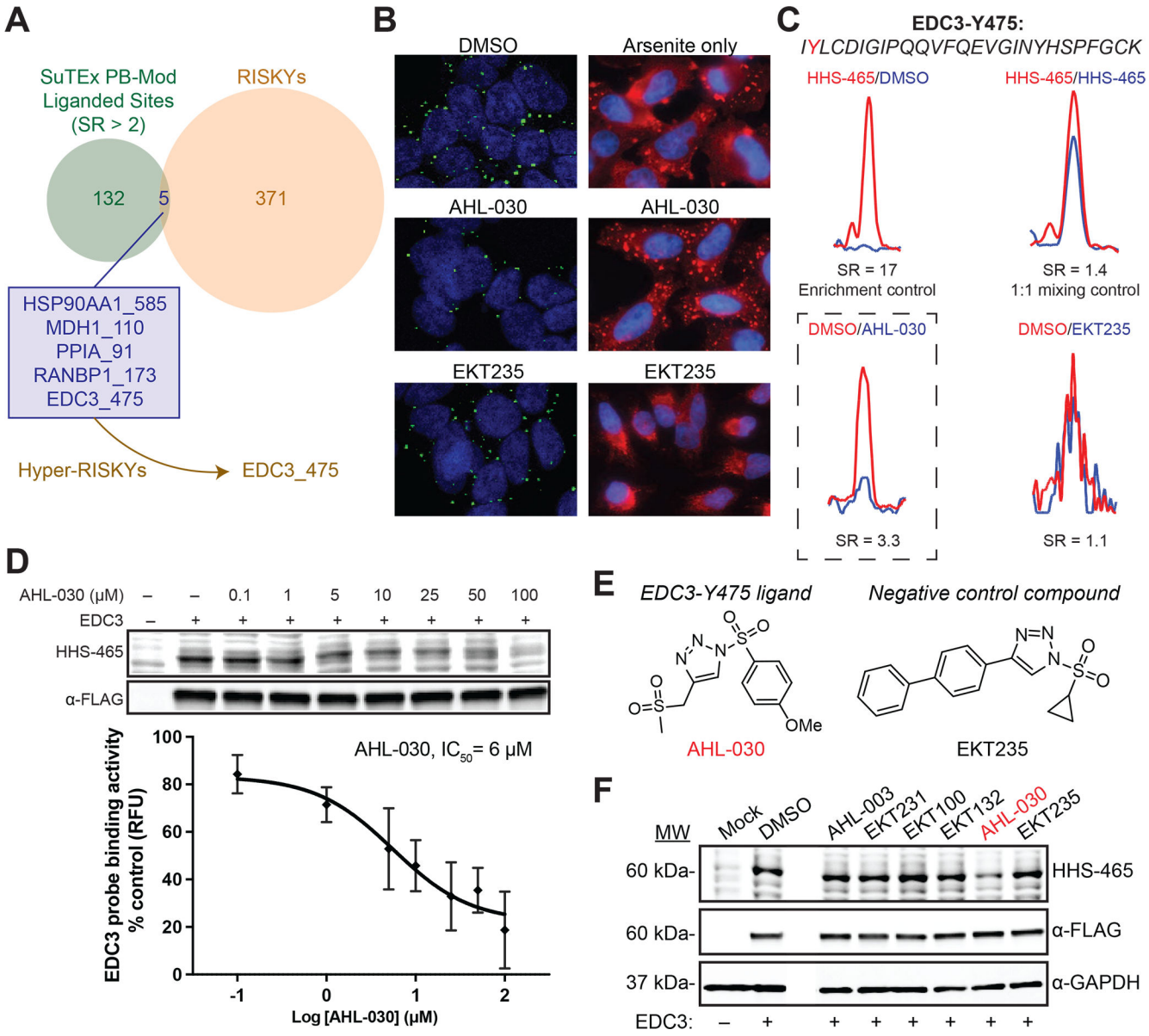

Figure 4. Discovery of a SuTEx ligand for the hyper-reactive EDC3 Y475 site.

(A) Overlap of liganded sites from SuTEx PB modulators with reported RNA granule induction-sensitive lysine and tyrosine sites (RISKYs[23a]). The five overlapping sites were further compared to previously reported hyper-RISKY sites[23a] resulting in the identification of the tyrosine-475 (Y475) site on EDC3. (B) Representative immunofluorescence images depicting decreased PBs and increased SGs in AHL-030-treated cells under stress conditions. EKT235 is shown as a negative control. See Figure S2 and S3 for additional details. (C) Representative MS1 extracted ion chromatograms (EICs) showing EDC3 Y475 is liganded by AHL-030 but not EKT235 [SILAC ratio or SR >2 for DMSO vehicle (light, red) / SuTEx fragment ligand (heavy, blue) treatment conditions]. Enrichment (HHS-465/DMSO) and 1:1 (HHS-465/HHS-465) controls are shown. SRs are calculated as the integrated area under the curve ratio of light-to-heavy peptide. SR values listed in Table

S4–6 are normalized to the 1:1 control for each respective probe-modified peptide. Data are representative of n = 2–3 biologically independent replicates. (D) Dose dependent inhibition of recombinant EDC3 probe labeling by AHL-030 *in situ*. EDC3-expressing HEK293T cells were pretreated with varying concentrations of AHL-030 (0.1 – 100 μM, 2 h) followed by lysis and probe labeling of soluble proteomes with HHS-465 (100 μM, 1 h, RT). The *in situ* IC_{50} for EDC3 probe labeling inhibition by AHL-030 was estimated to be ~6 μM. Comparable expression of recombinant EDC3 across treatment conditions was confirmed by western blots (α-FLAG). Data shown are mean ± SEM and representative of n = 3 biologically independent replicates. (E) Chemical structures of AHL-030 (left) and inactive control EKT235 (right). (F) Competitive gel-based ABPP analysis verifying AHL-030 (25 μM, 2 h) competition of HHS-465 probe labeling (100 μM, 1h, RT) of recombinant EDC3-HEK293T expressing cells under glucose-deprived conditions. SAR was demonstrated by lack of activity of other SuTEx compounds tested under the same treatment conditions. Western blots comparing recombinant expression of EDC3 (α-FLAG) and loading controls (α-GAPDH) are shown. Data are representative of n = 2 biologically independent replicates.

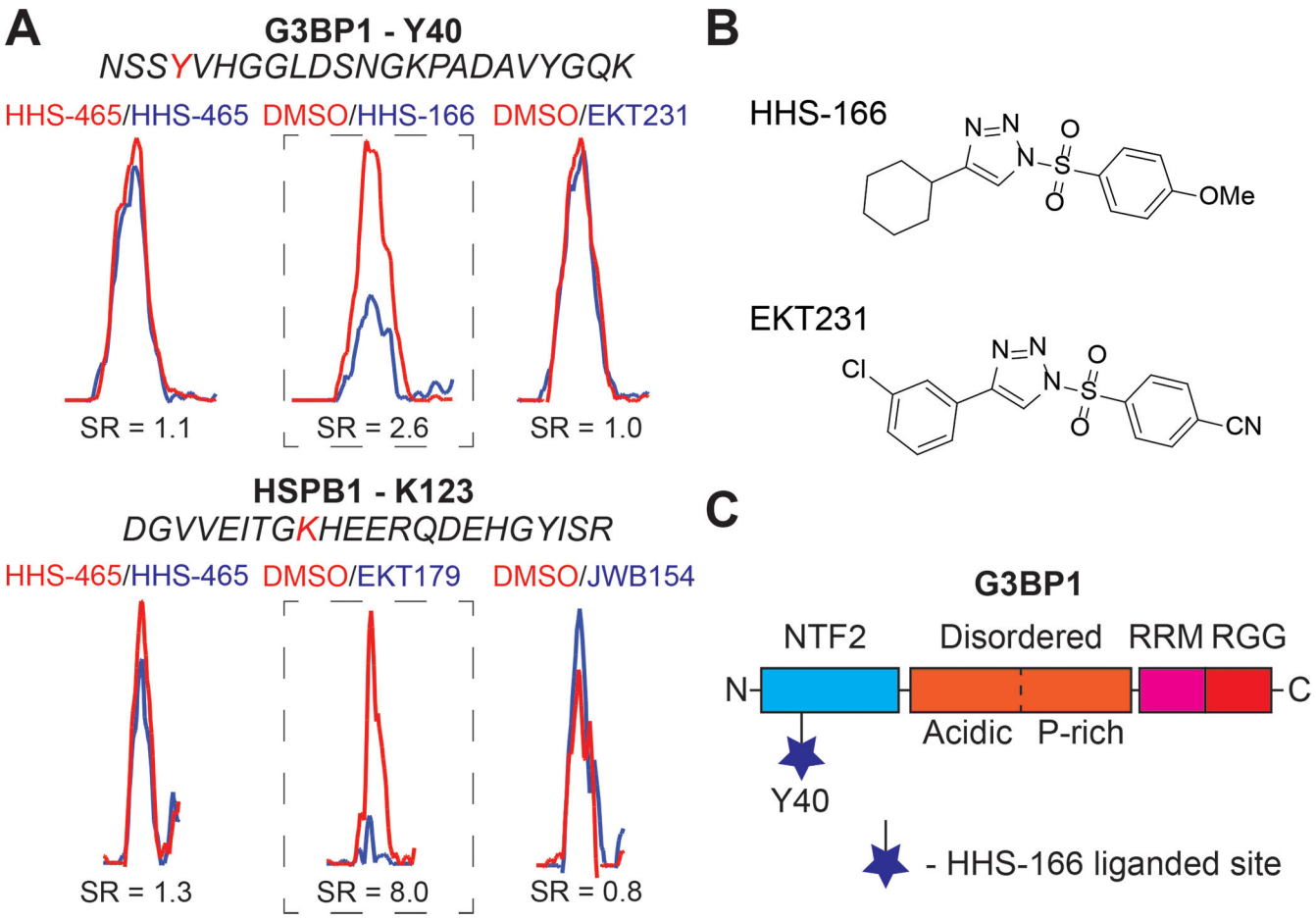

Figure 5. Discovery of a G3BP1-targeting SuTEx ligand.

(A) The SG-modulating SuTEx compounds HHS-166 and EKT179 ligand G3BP1 (Y40) and HSPB1 (K123), respectively, as determined by a SILAC ratio (SR) >2 for DMSO vehicle (light, red) compared with SuTEx fragment ligand (heavy, blue) treatment conditions. The lack of binding activity of structurally related compounds (EKT231 and JWB514) provide evidence for structure-activity relationship. A 1:1 SILAC mixing control (HHS-465/HHS-465) is shown and used for normalization. Representative MS1 extracted ion chromatograms (EICs) are shown. (B) The chemical structure of G3BP1 Y40 SuTEx ligand (HHS-166) and matching inactive control compound (EKT231). (C) G3BP1 domains showing the liganded Y40 site located in the NTF2 dimerization domain. Data are representative of $n = 2–3$ biologically independent replicates.

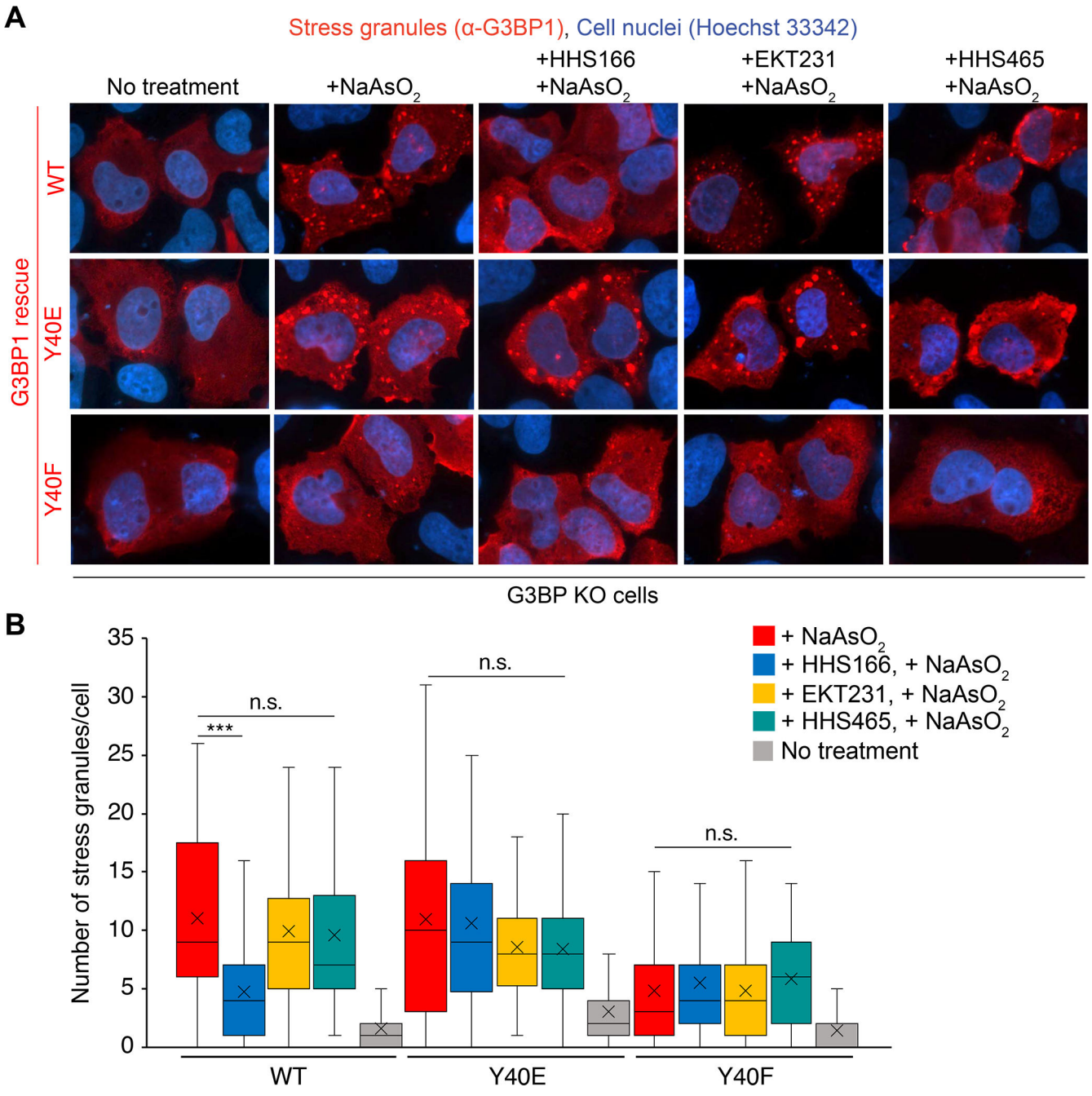

Figure 6. G3BP1 Y40 mediates the SG-modulating activity of HHS-166.

(A) G3BP1 and G3BP2 knockout (G3BP KO) cells rescued with G3BP1 wild-type (WT) or mutants exhibit differential sensitivity to SuTEx fragment treatment in arsenite-induced SG formation (α-G3BP1) as determined by immunofluorescence analysis. Expression of WT recombinant G3BP1 and Y40E mutant but not the Y40F mutant rescued the deficient arsenite-induced SG formation phenotype of G3BP KO cells. Arsenite-mediated SG formation was blocked by pretreatment with HHS-166 but not the inactive control compound EKT231 in G3BP1 WT- but not Y40E-, which lacks a tyrosine for covalent binding at this site, rescued G3BP KO cells. (B) Box and whisker plot of the number

of stress granules per cell from immunofluorescence images of G3BP KO rescue with G3BP1 WT/mutant + SuTEx fragment ligand treatments in arsenite-stressed cells from **A** ("x" indicates the mean; the center line is the median). Pretreatment with HHS-166 in G3BP1 WT-expressing G3BP KO cells resulted in a statistically significant decreases in SG formation (***$p < 0.001$, n.s.: not significant). A two-sample Student's t-test was performed for statistical comparison. Data shown are representative of $n = 3$ biologically independent replicates.